Inorganica Chimica Acta 374 (2011) 205–210

Contents lists available at ScienceDirect

Inorganica Chimica Acta

journal homepage: www.elsevier.com/locate/ica

Dbf–ruthenocenes: Towards chiral halfsandwich Lewis acidic Dbf complexes

Frank Pammer, Yu Sun, Werner R. Thiel *

FB Chemie, Technische Universität Kaiserslautern, Erwin-Schrödinger-Strasse, Geb. 54, 67633 Kaiserslautern, Germany

ARTICLE INFO

Article history:
Available online 21 March 2011

Dedicated to Prof. Dr. Wolfgang Kaim on the occasion of his 60th birthday.

Keywords:
Ruthenocenes
Dibenzofluorenide
X-ray structure

ABSTRACT

In order to develop a new class of chiral metallocene catalysts, halfsandwich ruthenocenes of dibenzo[*c,g*]fluorenide (Dbf^{-1}) have been prepared. Structural and spectroscopic characterization of (η^5-Dbf)Ru(PPh_3)$_2$Cl and [(η^5-Dbf)Ru(PPh_3)$_2$(NCMe]$^+$[SbF_6]$^-$ provide evidence for strong metal–ligand binding in these sterically crowded complexes. In the solid state the complexes assume conformations ideal for transfer of the stereo information unto a prochiral substrate.

1. Introduction

Due to its molecular structure, allowing the "localization" of aromaticity in the five-membered and in two of the four six-membered rings, the dibenzo[*c,g*]fluorenide ligand (Dbf^{-1}) is capable of stabilizing transition metal centers almost as efficiently as the cyclopentadienide ligand (Cp^{-1}) does. In our investigations on this ligand system we were able to show the high stability of Dbf complexes with a series of examples and could elucidate the electronic structure of these compounds by studies on their reactivity and by means of theoretical calculations [1]. In addition to its electronic features, the dibenzo[*c,g*]fluorenide ligand is an intrinsically chiral Cp derivative, since it possesses a binaphthyl backbone. Although it readily racemizes at low temperature, studies on the catalytic activity of Dbf complexes are beneficial due to the fact that substituting the hydrogen atoms in the 8- and 8′-positions results in conformationally stable Dbf analogs. Since ruthenium catalyzes a series of (enantioselective) transformations we therefore were interested in the synthesis and characterization of Dbf complexes of this metal.

Fluorenyl (Flu) complexes of ruthenium have only scarcely been described in literature. Aside from η^1-fluorenide complexes [2], and the sandwich compounds (Cp^*)Ru(Flu) [3,4] (Cp^*: 1,2,3,4,5-pentamethylcyclopentadienyl) and (Cp^*)Ru(Flu^*) [5], (Flu^*: 1,2,3,4,5,6,7,8,9-nonamethylfluorenyl) and a (η^5-Flu)(η^6-cymene) complex [6] only few η^5-fluorenide ruthenium complexes have been reported [7], including an *ansa*-carborane compound [8]. One recent development in metallocene chemistry is the application of cationic halfsandwich complexes of the group VIII-metals iron and ruthenium in asymmetric catalysis. In the past two decades a number of Lewis-acid catalysts with chiral phosphane ligands have been synthesised that facilitate enantioselective Diels–Alder-reactions [9]. Herein we report the synthesis and structural characterization of ruthenium halfsandwich complexes bearing the dibenzo[*c,g*]fluorenide ligand (Dbf^{-1}), which can be considered as precursors for the development of chiral organometallic ruthenium based Lewis acid-catalysts.

2. Experimental

2.1. General remarks

Elemental analyses were carried out at the Department of Chemistry (TU Kaiserslautern). Infrared spectra were recorded with a Perkin–Elmer FT-IR 1000 spectrometer. NMR spectra were recorded with a Bruker Avance 400 spectrometer. The assignment of the NMR data is according to Scheme 1. All reactions were carried out under an atmosphere of dinitrogen.

2.2. Chloro(η^5-dibenzo[c,g]fluorenide) triphenylphosphineruthenium(II) (**1**)

66.6 mg (250 μmol) of DbfH were dissolved in 5 ml of dry toluene in a Schlenk vessel. The solution was cooled to −15 °C and 172 μl of *n*-butyllithium (275 μmol, 1.6 M in hexane) was added drop-wise. While slowly warming to ambient temperature, the solution was stirred for 3 h. A colorless precipitate of (Dbf)Li formed during this time. This suspension was stirred at ambient temperature while 239.7 mg (250 μmol) of finely powdered

* Corresponding author. Tel.: +49 631 2052752; fax: +49 631 2054676.
E-mail address: thiel@chemie.uni-kl.de (W.R. Thiel).

0020-1693/$ - see front matter © 2011 Elsevier B.V. All rights reserved.
doi:10.1016/j.ica.2011.03.038

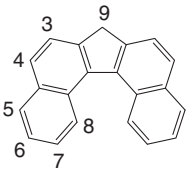

Scheme 1. Numbering of the NMR spectra.

$Ru(PPh_3)_3Cl_2$ [15] and another 15 ml of dry toluene were added. The initially formed brown suspension turned to red within 20 min. The reaction mixture was stirred for another 20 h, was filtered and the residue was extracted with another 5 ml of dry toluene. The obtained dark red solution was concentrated and brought to crystallize at −40 °C. The mother liquor was removed via a cannula and the remaining crystals were washed with a mixture of toluene/pentane (1:5, v:v). Three crops of dark red crystals were gathered by repeated concentration of the mother liquor and cooling to −40 °C. The product obtained in this fashion contained two equivalents of solvent ((Dbf)$Ru(PPh_3)_2Cl$·2 toluene). A total of 110 mg of product were isolated. Taking the solvent into account this amounts to a yield of 99 μmol, 40%. Single crystals for characterization by X-ray diffraction were obtained from the third crystallization fraction at −40 °C. The complex could also be purified by layering a solution in CH_2Cl_2 with pentane. The microcrystalline material obtained in this fashion did not contain solvent, but was not suitable for X-ray diffraction. ^{1}H NMR (400 MHz, $CDCl_3$, 293.5 K): δ [ppm] = 9.27 (d, 2H, $^3J_{HH}$ = 8.3 Hz, 8,8′-H), 7.69 (t, 2H, $^3J_{HH}$ = 7.3 Hz, 7,7′-H), 7.47 (t, 2H, $^3J_{HH}$ = 7.4 Hz, 6,6′-H), 7.32 (d, 2H, $^3J_{HH}$ = 7.2 Hz, 5,5′-H), 7.00-7.22 (br m, 18H, PPh_3: o-H/p-H), 6.70–6.92 (br, 12 H, PPh_3: m-H), 6.68 (d, 2H, $^3J_{HH}$ = 8.9 Hz, 3,3′/4,4′-H), 6.37 (d, 2H, $^3J_{HH}$ = 8.9 Hz, 3,3′/4,4′-H), 3.88 (s, 1H, 9-H). ^{1}H NMR (400 MHz, $CDCl_3$, 325.4 K): δ [ppm] = 9.30 (d, 2H, $^3J_{HH}$ = 8.3 Hz, 8,8′-H), 7.69 (t, 2H, $^3J_{HH}$ = 7.9 Hz, 7,7′-H), 7.48 (t, 2H, $^3J_{HH}$ = 7.4 Hz, 6,6′-H), 7.34 (d, 2H, $^3J_{HH}$ = 7.7 Hz, 5,5′-H), 7.11-7.20 (m, 12H, PPh_3: o-H), 7.05 (t, 6H, $^3J_{HH}$ = 7.2 Hz, PPh_3: p-H), 6.84 (t, 12H, $^3J_{HH}$ = 7.3 Hz, PPh_3: m-H), 6.70 (d, 2H, $^3J_{HH}$ = 8.9 Hz, 3,3′/4,4′-H), 6.34 (d, 2H, $^3J_{HH}$ = 8.9 Hz, 3,3′/4,4′-H), 3.90 (s, 1H, 9-H). ^{13}C NMR (100 MHz, $CDCl_3$, 293.5 K): δ [ppm] = 134.4 (br), 133.3, 132.1 (d, J_{PC} = 9.9 Hz), 131.7, 131.6, 129.3, 126.6 (d, J_{PC} = 12.2 Hz), 128.4 (br), 126.9 (t, J_{PC} = 4.4 Hz), 126.1, 124.8, 120.1, 108.4 (η^5-C), 94.2 (t, J_{PC} = 3.1 Hz, η^5-C), 56.2 (9-CH). ^{31}P NMR (162 MHz, $CDCl_3$, 293.5 K): δ [ppm] = 48.40. ^{31}P NMR (162 MHz, CD_2Cl_2, 293.5 K): δ [ppm] = 47.86. IR (KBr): ν [cm^{-1}] = 3051 (m), 2916 (w), 1615 (br, m), 1585 (w), 1571 (w), 1495 (w), 1481 (m), 1456 (w), 1433 (s), 1313 (w), 1262 (w), 1247 (w), 1189 (w), 1157 (w), 1118 (w), 1086 (m), 1049 (w), 1029 (w), 999 (w), 937 (w), 853 (w), 827 (w), 799 (m), 758 (w), 740 (m), 730 (w), 695 (s), 621 (w), 530 (w), 521 (s), 499 (w), 490 (w), 465 (m), 433 (w), 424 (w). MALDI-TOF MS: m/z = 629.256. Calcd.: ($C_{39}H_{38}PRu$) = [(Dbf)$Ru(PPh_3)$]$^+$ = 629.10. Mp: decomposition above 110 °C. Elemental *Anal.* Calc. for: $C_{57}H_{43}ClP_2Ru$: C, 73.90; H, 4.68, exp.: C 73.65, H 5.13.

2.3. (Acetonitrile)(η^5-dibenzo[c,g]fluorenide) triphenylphosphineruthenium(II) hexafluoroantimonate (**2**)

Forty milligrams of (Dbf)$Ru(PPh_3)_2Cl$·(C_7H_8)$_2$ (36 μmol) were dissolved in 10 ml of dry CH_2Cl_2 in a Schlenk tube. Dry acetonitrile (0.1 ml) was added, the reaction mixture was cooled to 0 °C and 12.4 mg (36.3 mmol) $AgSbF_6$ were added as a solid. While slowly warming to ambient temperature the red solution was stirred overnight. Subsequently the precipitate of AgCl was filtered off and the orange-red solution was concentrated until crystallization set in. The product was isolated by cooling the concentrated solution to −40 °C to yield 37.1 mg of the complex as orange red crystals suitable for X-ray diffraction. The crystalline material contains half an equivalent of CH_2Cl_2 and an additional 1.5 equivalents of acetonitrile. Taking into account the solvents of crystallization, this amounted to a yield of 29.2 μmol (81%). Alternatively **2** can be purified by layering a solution of the complex in CH_2Cl_2 with Et_2O. The crystalline material obtained in this fashion is bright red in color and contains half an equivalent of CH_2Cl_2 and Et_2O each. Yield: 37.1 mg (29.2 μmol, 81%). ^{1}H NMR (400 MHz, $CDCl_3$, 293.5 K): δ [ppm] = 9.07 (d, 2H, $^3J_{HH}$ = 8.3 Hz, 8,8′-H), 7.88 (t, 2H, $^3J_{HH}$ = 7.7 Hz, 7,7′-H), 7.61 (t, 2H, $^3J_{HH}$ = 7.5 Hz, 6,6′-H), 7.42 (d, 2H, $^3J_{HH}$ = 7.8 Hz, 5,5′-H), 7.21 (t, 6H, $^3J_{HH}$ = 7.3 Hz, PPh_3: p-H), 6.98 (t, 12H, $^3J_{HH}$ = 7.6 Hz, PPh_3: m-H), 6.86 (d, 2H, $^3J_{HH}$ = 8.9 Hz, 3,3′/4,4′-H), 6.76–6.84 (m, 12H, PPh_3: o-H), 6.16 (d, 2H, $^3J_{HH}$ = 8.9 Hz, 3,3′/4,4′-H), 4.21 (s, 1H, 9-H), 2.25 (s, 3H, NCMe). ^{13}C NMR (100 MHz, $CDCl_3$, 293.5 K): δ [ppm] = 107.9 (η^5-C_5), 93.4 (η^5-C_5), 60.4 (9-CH), 4.9 (NCMe), the ^{13}C-resonanzes in the aromatic region could not be interpreted due to PC-coupling and signal broadening and slow decomposition of the complex. ^{31}P NMR (162 MHz, $CDCl_3$, 293.6 K): δ [ppm] = 49.84. IR (KBr): ν [cm^{-1}] = 3141 (w), 3447 (m), 2973 (w), 2925 (w), 2865 (w), 2265 (w), 1967 (br w), 1903 (br w), 1827 (br w), 1777 (br w), 1615 (w), 1586 (w), 1574 (w), 1542 (w), 1512 (w), 1499 (w), 1480 (s), 1435 (s), 1313 (m), 1266 (w), 1247 (w), 1210 (w), 1184 (m), 1160 (w), 1118 (w), 1089 (s), 1027 (m), 1000 (m), 936 (w), 920 (w), 858 (m), 806 (m), 744 (s), 697 (s), 658 (s), 625 (w), 581 (w), 530 (s), 521 (s), 496 (s), 467 (w), 427 (m). MALDI-TOF MS: m/z = 629.256; calc. ($C_{39}H_{38}PRu$) = [(Dbf)$Ru(PPh_3)$]$^+$ = 629.10. Mp =

Table 1
Crystallographic data for **1** and **2**.

Compound	**1**	**2**
Formula	$C_{67.5}H_{51}Cl_2P_2Ru$	$C_{62.5}H_{51.5}ClF_6N_{2.5}P_2RuSb$
Formula weight	1060.54	1271.77
T (K)	150(2)	150(2)
Wavelength (Å)	1.54184 (Cu Kα)	0.71073 (Mo Kα)
Crystal size (mm)	0.20 × 0.11 × 0.08	0.58 × 0.26 × 0.17
Crystal system	monoclinic	triclinic
Space group	$P2_1/c$	$P\bar{1}$
a (Å)	20.5204(2)	11.0368(2)
b (Å)	11.95810(10)	21.8684(5)
c (Å)	20.9918(2)	23.8217(5)
α (°)	90	69.657(2)
β (°)	93.5910(10)	88.7380(10)
γ (°)	90	88.354(2)
V (Å^3)	5140.96(8)	5388.26(19)
Z	4	4
ρ_{calc} (g/cm^3)	1.370	1.568
μ (Cu Kα) (mm^{-1})	3.859	0.955
θ range (°)	4.26–62.67	4.02–32.41
Index ranges	$-23 \leqslant h \leqslant 22$, $-13 \leqslant k \leqslant 13$, $-23 \leqslant l \leqslant 24$	$-15 \leqslant h \leqslant 16$, $-28 \leqslant k \leqslant 32$, $-35 \leqslant l \leqslant 34$
Reflection collected	26 450	65 278
Unique reflections (R_{int})	8119 (0.0248)	33 835 (0.0282)
Absorption correction	semi-empirical from equivalents (multiscan)	
Data/restraints/parameters	8119/30/659	33 835/21/1374
Goodness-of-fit (GOF) on F^2	1.072	1.097
Final R indices [$I > 2\sigma(I)$][a]	R_1 = 0.0246, wR_2 = 0.0678	R_1 = 0.0577, wR_2 = 0.1727
R indices[a] (all data)	R_1 = 0.0288, wR_2 = 0.0691	R_1 = 0.0841, wR_2 = 0.1991
$\Delta\rho_{max/min}$ (e Å^{-3})	0.373/−0.508	6.819/−4.797

[a] $R_1 = \Sigma||F_o| - |F_c||/\Sigma|F_o|$; $wR_2 = \{\Sigma[w(F_o^2 - F_c^2)^2]/\Sigma[w(F_o^2)^2]\}^{1/2}$.

161–162 °C. Elemental *Anal.* Calc. for $C_{59}H_{46}F_6NP_2RuSb\cdot(^1/_2CH_2Cl_2)\cdot(^2/_3CH_3CN)$: C, 60.63; H, 4.05; N, 1.95. Found: C, 59.97; H, 3.82; N, 2.02%.

2.4. X-ray structure analyses

Single crystals of compounds **1** and **2** were carefully affixed with an adhesive onto the tips of glass fibers. The glass fibers were subsequently mounted on the goniometer head in a nitrogen stream at 150 K. Table 1 summarizes the cell parameters as well as the experimental details of the data collection and the structure refinements of both crystals. The structures were solved using direct method (SIR92) [10] and completed by subsequent difference Fourier syntheses, and refined by full-matrix least-squares procedures [11]. Semi-empirical absorption corrections from equivalents (Multiscan) were carried out [12]. All non-hydrogen atoms were refined with anisotropic displacement parameters. The quality of the crystals of compound **2** which were available for X-ray structure analysis was limited. The insufficient absorption correction left a high residual electron density around Sb1, the heaviest atom in the system. Additionally the counter-anion SbF_6^-, the un-coordinated co-solvents CH_3CN and CH_2Cl_2 were partially disordered. The disorder treatment of all these positions resulted in unstable refinements. However, in the structure of the cation $[(Dbf)Ru(PPh_3)_2(NCMe]^+$ no obvious abnormality was observed. All hydrogen atoms were placed in calculated positions and refined by using a riding model.

3. Results and discussion

The halfsandwich complex (η^5-Cp)$Ru(PPh_3)_2Cl$ can be obtained by heating $RuCl_3$ with PPh_3 in ethanol in the presence of an excess of cyclopentadiene (CpH) [13]. The formation of (η^5-Ind)$Ru(PPh_3)_2Cl$ [14] can be achieved in the same fashion, although the use of $Ru(PPh_3)_3Cl_2$ [15] as the starting material and the addition of KOH is necessary. By reaction of DbfLi with $Ru(PPh_3)_3Cl_2$ in dry toluene, the halfsandwich complex (η^5-Dbf)$Ru(PPh_3)_2Cl$ (**1**) can be isolated in satisfactory yield. It has to be pointed out that, due to the good solubility of $Ru(PPh_3)_3Cl_2$ in toluene, the reaction occurs in the neat solvent, without additional donors like THF or Et_2O (Scheme 2).

The complex can be isolated by crystallization either from a concentrated solution in toluene at −40 °C or by overlaying a solution of **1** in CH_2Cl_2 with pentane. The MALDI-TOF mass spectrum of the complex shows an intense signal around m/z = 629 that corresponds to the $[(Dbf)Ru(PPh_3)]^+$-fragment. The isotope pattern proves the presence of the presumed mononuclear ruthenium species (see Fig. 8 in Supplementary material). The $[(Dbf)Ru(PPh_3)_2]^+$ cation, which initially formed upon ionization by splitting off of the chloro ligand, is obviously not sufficiently persistent to be detected.

The PPh_3 ligands of **1** yield one signal in the ^{31}P NMR at 48.7 ppm ($CDCl_3$), which provides strong evidence for a rapid racemisation of the η^5-coordinated Dbf ligand. At ambient temperature signal broadening occurs in the ^1H NMR. Therefore ^1H NMR spectra have been recorded at 40 °C. The resonance of the 9-H proton of the Dbf ligand is observed at 3.90 ppm. Compound **1** is thus the only η^5-Dbf complex up to now that causes an upfield shift of the 9-H proton when compared to the free ligand DbfH (4.14 ppm in $CDCl_3$). The signals of the 8,8′-protons appear distinctly separated from the other aromatic resonances at 9.30 ppm (d, $^3J_{HH}$ = 8.3 Hz). Via *HH-COSY* NMR the 7,7′- and 6,6′-CH groups can be unambiguously assigned to triplets at 7.69 ppm ($^3J_{HH}$ = 7.9 Hz) and 7.48 ppm ($^3J_{HH}$ = 7.4 Hz), while the 5,5′-protons appear at 7.34 ppm (d, $^3J_{HH}$ = 7.7 Hz). The 3,3′- and 4,4′-protons yield doublets a 6.70 and 6.34 ppm. The phenyl groups of the phosphine ligands give three signal groups in the ^1H NMR spectrum. The *para*-protons yield a triplet at 7.05 ppm (6H, $^3J_{HH}$ = 7.2 Hz), the signals of the *meta*- and *ortho*-hydrogen atoms can then be can be assigned by *HH-COSY* NMR at 6.84 ppm (t, $^3J_{HH}$ = 7.7 Hz) and 7.11–7.20 ppm (m), respectively. In the ^{13}C NMR spectrum only the resonances of the carbon atoms of the η^5-coordinated ring can be identified at 56.2 ppm for the 9-CH group and at 91.2 and 108.4 ppm for the quaternary carbon atoms. The remaining aromatic resonances could not be interpreted due to line broadening, superposition and PC-coupling.

Single crystals of **1** for examination by X-ray diffraction were obtained by diffusion of pentane into a solution of the complex in toluene. Compound **1** crystallises as dark red prisms in the monoclinic space group $P2_1/c$ with four complex molecules and two molecules of toluene in the unit cell (Fig. 1). As the molecular structure shows, the bulky phosphine ligands impose a considerable steric strain on the Dbf moiety. The chiral ligand forms a relatively large torsion angle C10–C1–C11–C20 of 13.684(2)°, as compared to other η^5-Dbf complexes (minimum (η^5-Dbf)$Mn(CO)_3$: 10.75(5)° [1a], maximum (η^5-Dbf)(η^3-allyl)$Mo(CO)_3$: −15.6(13)° [1b]). This large torsion angle however does not correlate with the steric pressure of the PPh_3-groups, which causes a massive deformation of the Dbf framework and results in the closest approach of the 8,8′-protons yet observed (H9, H19 in Fig. 1, 1.9233 Å). The phosphine ligands are positioned "in front" of the Dbf ligand, thus evading the binaphthyl system. Still, two phenyl groups protrude beneath the naphthyl arms. The phenyl group

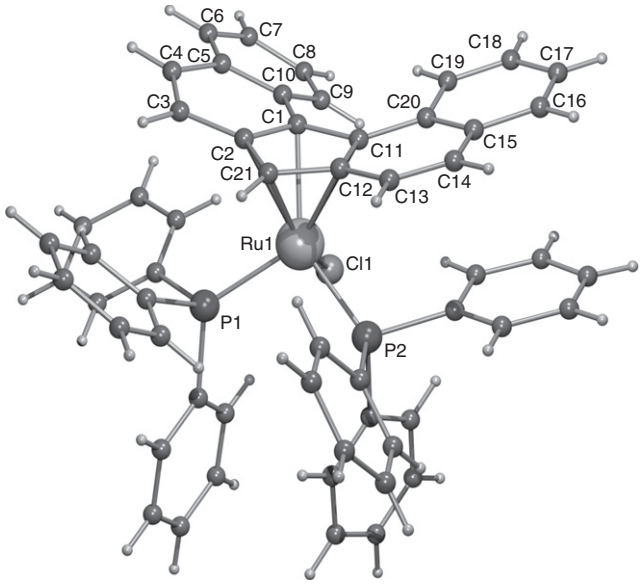

Fig. 1. Molecular structure of (η^5-Dbf)$Ru(PPh_3)_2Cl$ (**1**) in the solid state. The crystal structure contains two molecules of toluene, which have been omitted for clarity. Characteristic bond lengths (Å) and angles (°): Ru1–C1 2.317(2), Ru1–C2 2.339(2), Ru1–C21 2.199(2), Ru1–C12 2.265(2), Ru1–C11 2.331(2), Ru1–Ct1 1.9356, Ru1–Cl1 2.4330(5), Ru1–P1 2.3084(6) Ru1–P2 2.3074(5), C3–C4 1.341(3), C13–C14 1.343(3), H9–H19 1.9233 C10–C1–C11–C20 13.684(2).

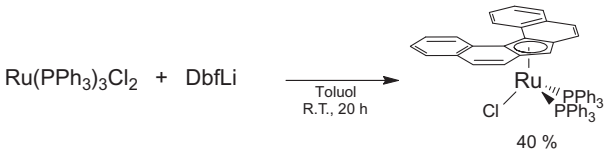

Scheme 2. Synthesis of (η^5-Dbf)$Ru(PPh_3)_2Cl$ starting from $Ru(PPh_3)_3Cl_2$.

containing the atoms C52–C53–C54–C55–C56–C57 assumes an almost co aligned conformation with respect to the C11–C12–C13–C14–C15–C20-ring in the upward bent naphthyl arm, as evidenced by an angle of only 2.484° between the two ring planes. A similar orientation is not found for the phenyl group interacting with the downward bent naphthyl arm. Instead, on order to avoid the steric pressure inflicted by the PPh_3 unit, the whole naphthyl system curves upward and twists, before bending down again. Quantitatively this deformation can be demonstrated by the positions of the protons H4, H6 and H9 relative to the five-membered ring C1–C2–C21–C12–C11. H4 and H6 are lifted by 1.0592 and 0.9083 Å above the ring plane, while H9 is located −0.9617 Å beneath.

The chloro ligand is positioned between the naphthyl groups 2.4330(5) Å from the ruthenium center, forming a dihedral angle Cl1–Ru1–C21–H21 of 150.494(1)°, thus deviating significantly from an ideal *trans* position. Curiously it has to be noted that the anion is shifted towards the downward pointing naphthyl arm. Furthermore several Cl–H contacts ranging from 2.6 to 3.2 Å (H53–Cl1 2.6454 Å, H39–Cl1 2.7728 Å, H27–Cl1 2.7798 Å, H47–Cl1 3.1714 Å) are found. With a Ru–Ct1 distance of 1.9356 Å the Dbf ligand is less closely bound to the metal than the indenyl fragment in (η^5-Ind)Ru(PPh_3)$_2$Cl (1.9175(2) Å) [16]. In the analogous Cp [17] and Cp* [18] complexes the distance between the metal center and ring plane is significantly smaller as well (1.8466(8) and 1.8875(2) Å). The deformation of the ligand backbone results in an unsymmetrical coordination of the five-membered ring to the central atom. While the quaternary carbon atoms C1, C2, and C11 exhibit surprisingly similar carbon–metal bond lengths (Ru1–C1 2.317(2) Å, Ru1–C2 2.339(2) Å, Ru1–C11 2.331(2) Å), the bonds to C21 and C12 appear significantly shortened in comparison (2.199(2) and 2.265(2) Å). Thus the ruthenium atom is shifted away from the ring center in direction to the bond C21–C12, due to the steric interaction of the P1–PPh_3 group with the downward pointing naphthyl moiety. The PPh_3 groups are located in almost identical distances from the metal center (Ru1–P1 2.3084(6) Å, Ru1–P2 2.3074(5) Å). The corresponding Ru–P bonds in CpRu(PPh_3)Cl and Cp*Ru(PPh_3)Cl were found to be 2–4 pm longer (CpRu(PPh_3)Cl: Ru–P 2.3366(11), 2.3353(9) Å; Cp*Ru(PPh_3)Cl: Ru–P 2.3449(6), 2.3363(6) Å). In (η^5-Ind)Ru(PPh_3)$_2$Cl two differing Ru–P bond length are found, due to the unequal steric interaction of the indenyl ring with the two phosphine moieties ((η^5-Ind)Ru(PPh_3)$_2$Cl: Ru–P 2.2681(5), 2.3306(6) Å), one being in the range of the Cp and Cp* complexes, while the other is even shorter than the Ru–P distances found for the Dbf complexes discussed here. The double bonds in position 3–4 and 3′–4′ appear to be significantly shortened, with bond lengths of C3–C4 = 1.341(3) Å and C13–C14 = 1.343(3) Å, respectively.

Since cationic complexes of the type [Cp(PPh_3)$_2$Ru(solv)]X (solv: coordinating solvent molecule; X: weakly coordinating anion) catalyze Diels–Alder reactions, we were interested in a similar system bearing the Dbf instead of the Cp unit. A number of such catalytically active cationic systems have been described [9]. The chloro ligand in (η^5-Dbf)Ru(PPh_3)$_2$Cl (**1**) can be cleaved off via a standard procedure by reacting (**1**) with $AgSbF_6$ in the presence of acetonitrile, to give the ionic compound [(Dbf)Ru(PPh_3)$_2$(NCMe)]$^+$[SbF_6]$^-$ (**2**) in over 80% yield (Scheme 3). The complex crystallizes well, but inevitably incorporates half an equivalent of dichloromethane as well as Et_2O or acetonitrile into the crystal lattice, depending on the crystallization procedure. Analogous compounds bearing indenyl- and cyclopentadienyl ligands such as ([(η^5-Ind)Ru(PPh_3)$_2$-(NCMe)]$^+$(BF_4^-) [19] and [(η^5-Cp)Ru(PPh_3)$_2$(NCMe)]$^+$(BF_4^-) [20]) are also known.

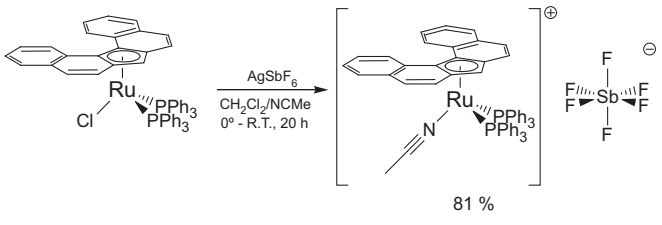

Scheme 3. Synthesis of [(Dbf)Ru(PPh_3)NCMe]$^+$(SbF_6)$^-$ (**2**).

The ^{1}H NMR spectrum in $CDCl_3$ proves the conversion of the complex. The signal of the 8,8′-protons has shifted as compared to the parent compound **1** (9.07 versus 9.30 ppm). The resonance of the 9-H group is now observed at 4.21, 0.3 ppm downfield from where the corresponding signal for **1** is found (3.90 ppm). Curiously, the resonances in the ^{31}P NMR are not affected by the ligand exchange. The complex exhibits a ^{31}P resonance at 49.8 ppm ($CDCl_3$), ((η^5-Dbf)Ru(PPh_3)$_2$Cl: 48.7 ppm, $CDCl_3$), which again proves the rapid racemisation of the η^5-coordinated Dbf ligand at room temperature. The ^{13}C NMR resonances of the five-membered ring can be easily assigned to signals at 107.9 and 93.4 ppm for the quaternary carbon atoms and 60.4 for the carbon atom of the 9-CH group. The coordinated molecule of acetonitrile can be identified by NMR spectroscopy as well. The signal of the methyl group is detected in the ^{1}H NMR spectrum at 2.25 ppm, thus being shifted downfield by 0.15 ppm as compared to the free molecule in solution. The effects of coordination are even more prominent in the ^{13}C NMR spectrum: here resonances at 4.9 ppm, for the methyl group and at around 130 ppm for the nitrile carbon atom were observed (free acetonitrile: 1.9, 116.4 ppm). The nitrile resonance could not be individually assigned, due to signal broadening and PC-coupling. Nevertheless, a correlation signal in the *HMBC*-NMR spectrum of the complex unambiguously identifies the quaternary carbon atom connected to the above mentioned methyl group (see Fig. 15 in the Supplementary material).

The complex crystallizes in the triclinic space group $P\bar{1}$. There are two crystallographically independent molecules present in the unit cell. The two structures – in the following referred to as α and β – differ only slightly from one another and will thus be discussed together. In the solid state the cationic molecules form layers with the SbF_6^- counteranions. Further remaining cavities in the crystal lattice are occupied by solvent molecules, amounting to 0.5 equivalents of CH_2Cl_2 and 1.5 equivalents of acetonitrile per complex molecule. The structure of one of the cations [(Dbf)Ru(PPh_3)$_2$(NCMe)]$^+$ in the solid state is presented in Fig. 2.

The solid state structure of **2** is similar to the structure found for **1**: the PPh_3 ligands assume positions on the side of the complex that not shielded by the Dbf-system, while the acetonitrile is found in between the two naphthyl moieties. As has been observed for the chloro complex, the acetonitrile group is not coordinated in a symmetrical way. Instead a noticeable shift towards the downward pointing naphthyl arm is found, leading to a dihedral angle H21–C21–Ru1–N1 of −150.948(6)° (**2**-α, **2**-β: H81–C81–Ru2–N2 −146.477(7)°). Accordingly the angles between the ruthenium, nitrogen atom and the nitrile carbon atoms C58 deviate significantly – by 9–10° – from the ideal value: **2**-α, Ru1–N1–C58 = 169.841(4)°; **2**-β, Ru2–N2–C118 = 170.895(4)°. The distances of the nitrogen atoms from the ruthenium centers are slightly longer than in the corresponding Cp complex Ru1–N1 = 2.047(3) Å (**2**-α, **2**-β: Ru2–N2 = 2.050(3) versus 2.0412(40) Å). It has to be noted, that the triple bonds of the acetonitrile ligands are longer than expected for a noncoordinating nitrile (C–C≡N: 1.136 Å [21], **2**-α: N1–C58 1.150(5) Å, **2**-β: N2–C118 1.144(5) Å), while the corresponding bond in the Cp analog [(η^5-Cp)Ru(PPh_3)$_2$(NCMe)]BF_4 was found to be significantly shorter (1.1283 Å) [20]. The ruthenium-phosphorus bonds in **2**-α (Ru1–

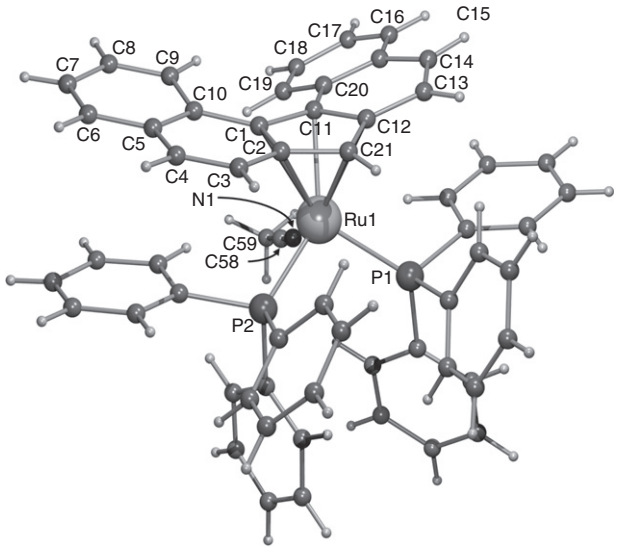

Fig. 2. Molecular structure of one of the cations $[(Dbf)Ru(PPh_3)_2(NCMe)]^+$ in the solid state. The crystal structure contains additional solvent molecules and anions, which have been omitted for clarity. Characteristic bond lengths (Å) and angles (°): Ru1–C1 2.344(4), Ru1–C12 2.344(4), Ru1–C2 2.278(4), Ru1–C11 2.300(4), Ru1–N1 2.047(3), Ru1–P2 2.3233(10), Ru1–P1 2.3323(10), Ru1–C21 2.214(4), C3–C4 1.353(6), C13–C14 1.343(6), P1–Ru1–P2 95.72(4), P1–Ru1–N1 92.70(9), P2–Ru1–N1 92.50(9) Ru1–N1–C58 169.8(3).

P1 2.3323(9) Å, Ru1–P2 2.3233(10) Å) and **2**-β (Ru2–P3 2.3235(9) Å, Ru2–P4 2.3302(9) Å) are elongated by 1.5–2.5 pm as compared to $(Dbf)Ru(PPh_3)_2Cl$ (Ru1–P1 2.3084(6) Å, Ru1–P2 2.3074(5) Å). The torsion angles of the binaphthyl systems C10–C1–C11–C20 and C70–C61–C71–C80 yield different values for the two conformers (**2**-α: −14.654(9)°, **2**-β: −17.696(9)°) and in consequence lead to different distances between 8,8′-protons H9–H19 (1.9534 Å) and H69–H79 (2.0063 Å). In spite of the larger torsion angle the deformation of the ligand backbone appears to be less pronounced in **2** than in $(Dbf)Ru(PPh_3)_2Cl$. For example in the downward pointing naphthyl arms the H14 and H16 (**2**-α, **2**-β: H74, H76) are lifted by 0.8703 and 0.5105 Å (0.9141 and 0.5507 Å) above the corresponding planes of the five-membered rings ($(Dbf)Ru(PPh_3)_2Cl$: H4 1.0592 Å, H6 0.9083 Å). The twist of the terminal phenylene rings also is less pronounced. The distance of the η^5-C_5 rings from the metal centers is almost identical in **2**-α and **2**-β (Ru1–Ct1 1.9402 Å and Ru2–Ct2 1.9449 Å), but slightly larger than in the starting material (Ru1–Ct1 1.9356 Å). The metal-centroid distance surpasses the corresponding value in $[(\eta^5\text{-Cp})Ru(PPh_3)_2(NCMe)]BF_4$ by almost 10 pm (1.8480(3) Å). We attribute this to the far smaller steric interaction of the Cp ligand with the PPh_3 groups, as compared to Dbf. This assumption is corroborated by the

fact, that in the more sterically crowded indenyl complex $[(\eta^5\text{-Ind})Ru(PPh_3)_2(NCMe)]BF_4$ [19] intermediate Ru–Ct distances are found (1.8926(6) and 1.8791(6) Å). The shift of the metal center out of the Dbf ring center, which has been observed for $(Dbf)Ru(PPh_3)_2Cl$ also occurs in **2**-α and **2**-β. In **2**-α, the metal–carbon bonds to C21 and C2 are shortened to 2.215(4) and 2.278(3) Å, respectively. The three remaining carbon-metal bonds are longer (Ru1–C11 = 2.300(3) Å, Ru1–C1 = 2.344(3) Å, Ru1–C12 2.344(3) Å). In **2**-β the bond lengths differ less, due to more pronounced torsion of the binaphthyl system: the bonds to the nuclei equivalent to C21 and C2 (C81, C62) are shortened to 2.219(3) and 2.289(3) Å, while the bonds to C61 and C72 are elongated to 2.339(3) and 2.351(3) Å. The bond between the ruthenium center and C71 is shortened to 2.286(3) Å due to the deformation of the ligand backbone.

In both complexes discussed above, the sterically demanding PPh_3 ligands assume positions opposite to the binaphthyl system, leaving only the coordination position beneath the binaphthyl system for the remaining fourth ligand. In this position the substrate of a to-be-synthesised catalytically active complex must be coordinated (e.g. acroleine). Due to the torsion of the binaphthyl system, one enantiofacial side of the substrate would always be shielded more effectively than the other. This should allow the catalyst to differentiate between the two enantiotopic sides. Therefore complexes like **2** can be used as Lewis-acid-catalysts directly. However, it has been shown, that yields and enantioselectivities achieved with acetonitrile complexes are often unsatisfactory. Much better results are obtained when the adduct of the complex with an aldehyde is used [9a]. The substitution of the chloro ligand or the acetonitrile group by acroleine was not successful for **1** and **2** up to now.[1]

Compound **2** showed no catalytic activity in [4 + 2]-cycloaddition of acroleine to cyclopentadiene, which is a standard reaction for Diels–Alder catalysts. This may be attributed to the massive steric crowding of the active center, which inhibits the displacement of the acetonitrile ligand and the approach of reaction partners to the substrate. It is also possible, that the PPh_3 ligands are too basic, thus lower the Lewis acidity of the metal center beneath the activity threshold. As mentioned by Kündig [9h,i] electron rich phosphines can inhibit catalytic activity. Much better results might therefore be achieved with perfluorinated phosphites.

4. Conclusion

Treatment of $(PPh_3)_3RuCl_2$ with LiDbf results in the formation of $(\eta^5\text{-Dbf})Ru(PPh_3)_2Cl$. The chloro ligand can be exchanged against an acetonitrile ligand by reacting this compound with $AgSbF_6$ in the presence of acetonitrile leading to the ionic compound $[(Dbf)Ru(PPh_3)_2(NCMe)]^+[SbF_6]^-$. The η^5-coordinated Dbf ligands undergo rapid racemization in both cases. However, in both solid state structures, the chiral conformation of the Dbf ligand is frozen. We are presently working on stereochemically stable Dbf derivatives which may open up a new concept for enantioselective catalysis.

Appendix A. Supplementary material

CCDC 812240 and 812241 contain the supplementary crystallographic data for (**1**) and (**2**). These data can be obtained free of charge from The Cambridge Crystallographic Data Centre via www.ccdc.cam.ac.uk/data_request/cif. Supplementary data associated with this article can be found, in the online version, at doi:10.1016/j.ica.2011.03.038.

References

[1] (a) F. Pammer, Y. Sun, C. May, G. Wolmershäuser, H. Kelm, H.-J. Krüger, W.R. Thiel, Angew. Chem., Int. Ed. 46 (2007) 1270;
(b) F. Pammer, Y. Sun, W.R. Thiel, Organometallics 27 (2008) 1015;
(c) F. Pammer, Y. Sun, M. Pagels, D. Weismann, H. Sitzmann, W.R. Thiel, Angew. Chem., Int. Ed. 47 (2008) 3271;
(d) F. Pammer, Y. Sun, D. Weismann, H. Sitzmann, W.R. Thiel, Chem. Eur. J. 16 (2010) 1265;
(e) F. Pammer, Y. Sun, M. Sieger, J. Fiedler, B. Sarkar, W.R. Thiel, Organometallics 29 (2010) 6165.
[2] J. Yang, W.M. Jones, J.K. Dixon, N.T. Allison, J. Am. Chem. Soc. 117 (1995) 9776.
[3] (a) S. Luo, X. Zhao, B. Mu, H. Song, S. Xu, B. Wang, Organometallics 28 (2009) 4602;
(b) P.G. Gassman, J.R. Sowa Jr., M.G. Hill, K.R. Mann, Organometallics 14 (1995) 4879;

[1] Kündig [9b] describes acroleine adducts of Lewis-acid catalysts be only below −20 °C. We therefore tried to crystallise such a species a low temperatures, but no product could be isolated.

(c) M.F. Ryan, A.R. Siedle, M.J. Burk, D.E. Richardson, Organometallics 11 (1992) 4231.
[4] E. Kirillov, S. Kahlal, T. Roisnel, T. Georgelin, J.-Y. Saillard, J.-F. Carpentier, Organometallics 27 (2008) 387.
[5] P. Bazinet, K.A. Tupper, T.D. Tilley, Organometallics 25 (2006) 4286.
[6] G. Albertin, S. Antoniutti, F. Callegaro, J. Castro, Organometallics 28 (2009) 4475.
[7] (a) J.R. Fulton, S. Sklenak, M.W. Bouwkamp, R.G. Bergman, J. Am. Chem. Soc. 124 (2002) 4722;
(b) M. Buchmeiser, H. Schottenberger, Organometallics 12 (1993) 2472.
[8] Y. Sun, H.-S. Chan, P.H. Dixneuf, Z. Xie, Organometallics 23 (2004) 5864.
[9] (a) Y. Matsuo, Y. Mitani, Y.-W. Zhong, E. Nakamura, Organometallics 25 (2006) 2826;
(b) B.M. Trost, X. Huang, Org. Lett. 7 (2005) 2097;
(c) V. Alezra, G. Bernardinelli, C. Corminboeuf, U. Frey, E.P. Kündig, A.E. Merbach, C.M. Saudan, F. Viton, J. Weber, J. Am. Chem. Soc. 126 (2004) 4843;
(d) E.P. Kündig, C.M. Saudan, V. Alezra, F. Viton, G. Bernardinelli, Angew. Chem., Int. Ed. 40 (2001) 4481;
(e) E.P. Kündig, C.M. Saudan, F. Viton, Adv. Synth. Catal. 343 (2001) 51;
(f) E.P. Kündig, C.M. Saudan, G. Bernardinelli, Angew. Chem., Int. Ed. 38 (1999) 1220;
(g) M.E. Bruin, E.P. Kündig, Chem. Commun. (1998) 2635;
(h) E.P. Kündig, B. Bourdin, G. Bernardinelli, Angew. Chem. 106 (1994) 1931;
(i) A.S. Olson, W.J. Seitz, M.M. Hossain, Tetrahedron Lett. 32 (1991) 5299;
(j) J.W. Faller, C.J. Smart, Tetrahedron Lett. 30 (1989) 1189;
(k) S.G. Davies, J.C. Walker, J. Chem. Soc., Chem. Commun. (1986) 609;
(l) B.L. Booth, R.N. Haszeldine, N.I. Tucker, J. Chem. Soc., Dalton Trans. (1975) 1446.
[10] A. Altomare, G. Cascarano, C. Giacovazzo, A. Guagliardi, M.C. Burla, G. Polidori, M. Camalli, J. Appl. Cryst. 27 (1994) 435.
[11] G.M. Sheldrick, Acta Crystallogr., Sect. A 64 (2008) 112.
[12] CrysAlisPro, Oxford Diffraction Ltd., Version 1.171.32.5, 2007.
[13] M.I. Bruce, C. Hameister, A.G. Swincer, R.C. Wallis, Inorg. Synth. 21 (1982) 78.
[14] L.A. Oro, M.A. Ciriano, M. Campo, C. Foces-Foces, F.H. Cano, J. Organomet. Chem. 289 (1985) 117.
[15] T.A. Stephenson, G. Wilkinson, J. Inorg. Nucl. Chem. 28 (1966) 945.
[16] M. Kamigaito, Y. Watanabe, T. Ando, M. Sawamoto, J. Am. Chem. Soc. 124 (2002) 9994.
[17] M.I. Bruce, F.S. Wong, B.W. Skelton, A.H. White, J. Chem. Soc., Dalton Trans. (1981) 1398.
[18] I.A. Guzei, M.A. Paz-Sandoval, R. Torres-Lubian, P. Juarez-Saavedra, Acta Crystallogr. Sect., C: Cryst. Struct. Commun. 55 (1999) 1090.
[19] S.S. Keisham, Y.A. Mozharivskyj, P.J. Carroll, M.R. Kollipara, J. Organomet. Chem. 689 (2004) 1249.
[20] O.Y. Carreón, M.A. Leyva, J.M. Fernández, G.A. Pénicaud, Acta Crystallogr. Sect., C: Cryst. Struct. Commun. 53 (1997) 301.
[21] D.R. Lide (Ed.), CRC Handbook of Chemistry and Physics, 90th ed., Taylor and Francis Ltd., London, 2009.